Annu. Rev. Mater. Res. 2005. 35:505–38
doi: 10.1146/annurev.matsci.35.100303.110641

First published online as a Review in Advance on April 4, 2005

COMPOSITE MATERIALS FOR WIND POWER TURBINE BLADES

Povl Brøndsted, Hans Lilholt, and Aage Lystrup
Materials Research Department, Risoe National Laboratory, DK 4000 Roskilde, Denmark; email: povl.brondsted@risoe.dk, hans.lilholt@risoe.dk, aage.lystrup@risoe.dk

Key Words composites, properties, processing, damage, fatigue

■ **Abstract** Renewable energy resources, of which wind energy is prominent, are part of the solution to the global energy problem. Wind turbine and the rotorblade concepts are reviewed, and loadings by wind and gravity as important factors for the fatigue performance of the materials are considered. Wood and composites are discussed as candidates for rotorblades. The fibers and matrices for composites are described, and their high stiffness, low density, and good fatigue performance are emphasized. Manufacturing technologies for composites are presented and evaluated with respect to advantages, problems, and industrial potential. The important technologies of today are prepreg (pre-impregnated) technology and resin infusion technology. The mechanical properties of fiber composite materials are discussed, with a focus on fatigue performance. Damage and materials degradation during fatigue are described. Testing procedures for documentation of properties are reviewed, and fatigue loading histories are discussed, together with methods for data handling and statistical analysis of (large) amounts of test data. Future challenges for materials in the field of wind turbines are presented, with a focus on thermoplastic composites, new structural materials concepts, new structural design aspects, structural health monitoring, and the coming trends and markets for wind energy.

INTRODUCTION

The international wind energy market showed a new record in 2003 with a growth rate of 15%. Globally, a total power of 8.3 GW was installed. The total installed wind energy power has now reached more than 40 GW, and the average growth in the market during the past five years has been 26% per year. These figures were reported in the annual report on the status for wind energy in March 2004 from the consulting company BTM (1). This illustrates how during the past 25 to 30 years the use of wind turbines for electricity generation has grown from a grass-root initiative to an efficient alternative energy resource. The capacity of a commercial wind turbine has today reached the range of 2–5 MW, with large plants being built world-wide on land and offshore.

This status illustrates the increasing concern in the world, and perhaps in Europe in particular, about the supply and consumption of energy in a modern and civilized society. Over the centuries, energy has been supplied by wood, coke, coal, oil, and natural gas, as well as by uranium (nuclear energy). The early sources were natural in the sense that they renewed themselves over a short time period (years), while the later energy supplies were tapped from sources established millions of years ago. The increasing energy demands in the world today, owing to improved and expanded civilizations and to increasing populations, have led to concerns over the limited energy resources in storage on the earth.

At the same time there is an increasing concern about the pollution of the world/environment (generation of waste). This has led to the focus on a sustainable energy supply, which (probably) implies optimized use of energy, minimized pollution and, implicitly, reduction in energy consumption. These aspects have led to an increasing focus on the short-time stored energy resources; among these the most developed types today are wind energy and biomass (in various forms).

WIND ENERGY

For wind energy a converter is needed to turn the kinetic wind energy into operational energy, e.g., electricity and/or heat. The converter is based on a rotor driven by the wind, thereby extracting a power of

$$\mathrm{P} = \alpha \rho A v^3, \qquad 1.$$

where α is an aerodynamic efficiency constant, ρ the density of air, A the area of rotor-plane, and v the wind velocity. The rotor needs some sort of aerodynamic device, e.g., a wing or rotorblade with an aerodynamic shape, to be able to rotate. The rotor is typically placed on a tower, and this converter is usually called a wind turbine (in the past, a wind mill). In the early years the United States used the designation wind energy conversion system (WECS). Today nearly all wind turbines have rotors with three blades, where the rotor is mounted in an approximately vertical plane, on a horizontal axis, facing into the wind (Figure 1).

ROTORBLADES

The present review is focused on the rotorblades, which probably present the most challenging materials, design, and engineering problems. The rotor and its three rotorblades constitute a rather flimsy structure, consisting of cantilever-mounted blades on a central hub. The basic design aspects for a rotorblade are the selection of material and shape. The material should be stiff, strong, and light. The shape should be aerodynamic, similar to that of an airplane wing.

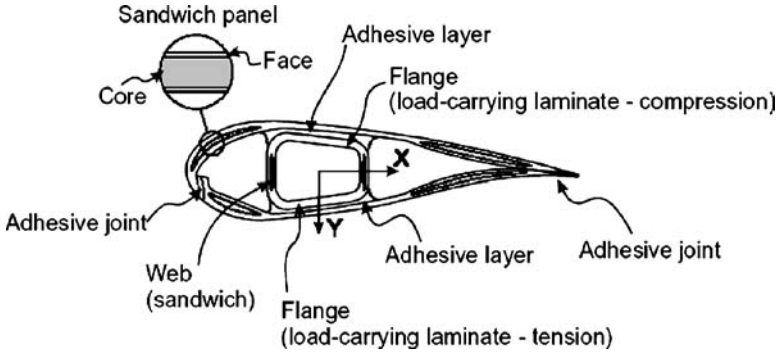

Figure 2 Cross-section principle of a rotorblade giving the nomenclature of the different blade construction elements.

The shape of a rotorblade in cross section is shown in Figure 2. The aerodynamic contours are formed by the (outer) relatively thin shells. They are supported structurally by a longitudinal beam or by webs, which carry a substantial part of the load on the blade. In the longitudinal direction, the rotorblades are tapered and twisted. The tapering is needed to economize with weight of the material because of the increasing loads from tip to root of a cantilever structure. The tapering, both in external shape and in thickness of the shells/beams/webs, is usually designed to ensure the same materials loadings, e.g., a maximum strain as design allowable.

It is interesting to note, as the pioneering work in the United States in 1970 (and earlier) observed, that a simple plank of constant cross-sectional area, rounded along the forward edge and sharpened along the rear edge, and with no twist of the (rectangular) profile, would have an aerodynamic efficiency of 75–80%, where 100% accounts for a rotorblade optimized according to the principles described above. The challenge for the designers is thus to go beyond the simple plank and integrate the aerodynamic shape, the tapering and the twist, into a design of the blade structure that is optimized with respect to materials selection and cost-effective production.

LOADS ON ROTORBLADES

The rotor and the rotorblades are exposed to external loads. These originate from the wind and from gravity. The general rotorblade geometry shown in Figure 2 has the blades arranged with their flat dimension in the plane of the rotor. This is so because the linear velocity of the outer part of the blade is high with blade tip speeds of 75–85 m/s, which are much higher than the wind speeds, even at storm conditions (~25 m/s). Therefore the relative wind direction, as seen by the blade, is nearly in the plane of the rotor, although the real wind direction is at a right angle to the rotor plane.

The blades are exposed to the wind that through the lift on the aerodynamic profile causes loads at right angle to the blades, which therefore react by bending flap-wise. These loads are both static, causing a permanent bending of the blades, and dynamic, causing a fatigue flap-wise bending because of the natural variations in wind speed. In addition, these static and fatigue load spectra vary during rotation, as seen by a given blade, when the blade points upward and downward, respectively; this is caused by the natural wind shear, which is the increase of average wind speed with increasing height over the terrain.

Normally, the maximum wind speed for operation of the wind turbine is about 25 m/s, i.e., storm conditions, beyond which the rotor is brought to a standstill by turning the rotorblades out of the wind by rotation about the longitudinal axis of the blade. This position exposes the rotorblades to the wind, coming in a right angle to blade planar surface, and causes the blade to bend as under a steady load on its surface. The natural variations in wind speed will cause dynamic flap-wise fatigue load spectra, as seen by the blade. The absolute magnitudes of these loads are comparable to the aerodynamic lift on the blades, as described above. Therefore, the rotorblades are exposed to flap-wise bending fatigue loads in varying spectra distributions under all conditions during service.

The blades are also exposed to gravity, and this is most pronounced when they are in their horizontal position. These loads cause bending in an edge-wise mode, and a given blade bends one way on the right-hand side and the opposite way on the left-hand side of rotor plane. This explains why the edge-wise bending also causes fatigue of the blade material and structure during rotation. Furthermore, the blades are exposed to centrifugal forces during the rotation of the rotor. Due to the limits of the linear blade velocity, the rotational speed is relatively low, typically from 20 rpm down to 10 rpm for large rotors/long rotorblades. Therefore, the longitudinal tensile loads in the blades are relatively low and normally are not taken into account as a design parameter. The design lifetime of modern wind turbines is normally thought to be 20 years, and the corresponding number of rotations is of the order 10^8 to 10^9.

MATERIALS REQUIREMENTS

These operational parameters and conditions lead to the following requirements focused on stiffness, density, and long-time fatigue:

- high material stiffness is needed to maintain optimal aerodynamic performance,
- low density is needed to reduce gravity forces,
- long-fatigue life is needed to reduce material degradation.

The optimal design of the rotorblades is today a complex and multifaceted task and requires optimization of properties, performance, and economy. It is not the objective of this review to discuss the design process in detail, but rather to focus

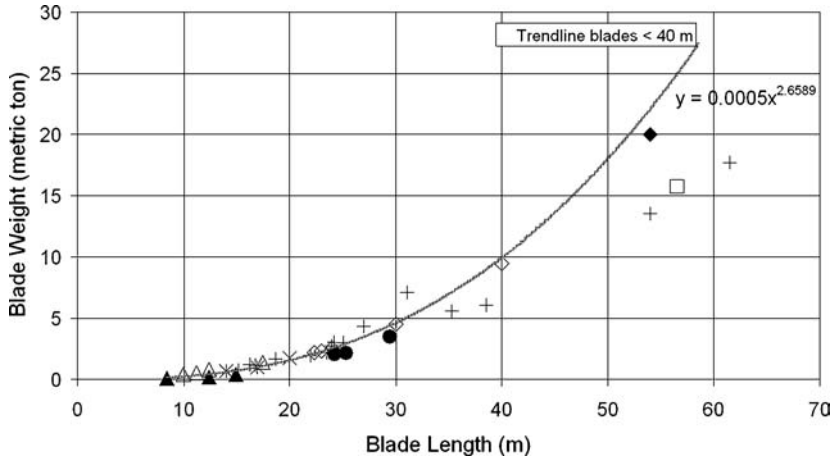

Figure 3 Development in rotorblade weight versus length. Symbols indicate different manufacturers and processing technologies.

on the materials and how they meet the requirements of wind turbine performance, as discussed above.

The combined result of the design process and the materials can be illustrated in the form of rotorblade weight as a function of rotorblade length, as presented in Figure 3. The lower end of the curve represents the relatively short blades of length 12–15 m, as were common in the early years of wind turbine design (1980s). The points represent rotorblades of increasing length, as developed until the present. An empirical curve is shown for the points representing blades with lengths below 40 m, giving a power law with an exponent of about 2.6; this is lower than expected for a simple up-scaling of the design on a volume basis (exponent 3), but it corresponds more closely to up-scaling of only two dimensions (length and thickness, exponent 2). This rather low exponent is a good indication of the high quality of the design process. Three recent and very long rotorblades of 54 to 61.5 m (2), plotted in Figure 3, show the further improvement in the design process by the points being below the extrapolated empirical curve, although it should be noted that they might refer to different wind load classifications. An additional discussion of these recent design improvements is given below.

The materials properties requirements of high stiffness, low weight, and long-fatigue life can be used to perform a materials selection, initially looking at all materials. The property combinations presented in Reference (3) are illustrative for a first selection of potentially usable materials classes. In a simplified form, the diagram of stiffness versus density in Figure 4 shows the procedure to be used (4). For details of materials selection, see Reference (3). The mechanical design of a rotorblade corresponds nominally to a beam, and the merit index is for this case

$$M_b = E^{1/2}/\rho, \qquad 2.$$

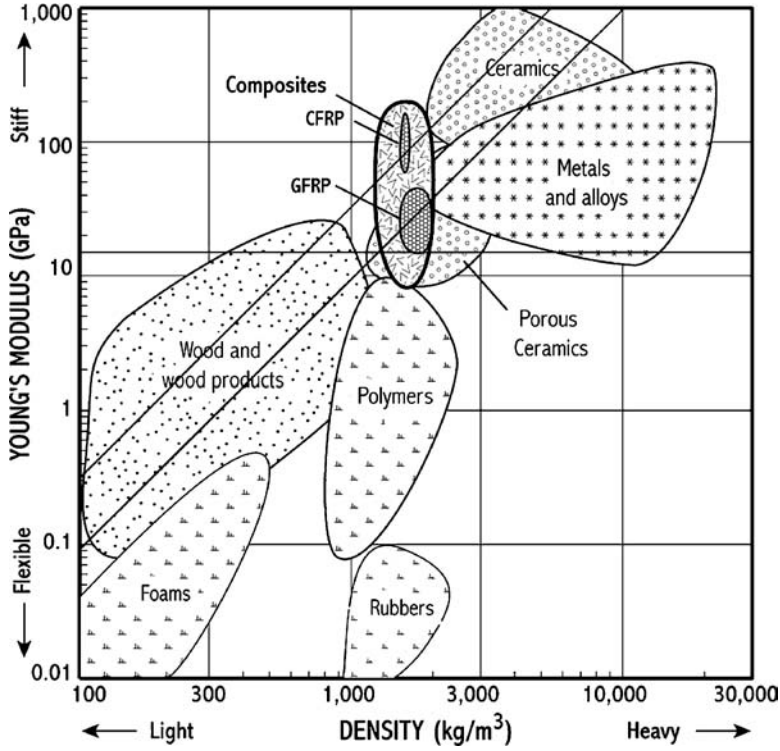

Figure 4 Diagram showing stiffness versus density for all materials. The merit index for a beam $M_b = E^{1/2}/\rho$ is represented by sloping lines with M_b equal to 0.003 (*lower line*) and 0.006 (*upper line*). The criterion for absolute stiffness E = 15 GPa is indicated by the horizontal line (4).

where E is the material stiffness and ρ is the material density. Lines of constant M_b are superimposed on the diagram, and materials that fulfill the criterion (partially or completely) are on the line and to the upper-left of the line.

The two lines shown in Figure 4 are arbitrary and illustrate lines of materials that are equally good in terms of stiffness and density for a cantilever beam. The lower of the two lines indicates that potential candidates materials are wood, composites, porous ceramics, metals, and ceramics. The lower line has a merit index of $M_b = 0.003$ with units of E in GPa and ρ in kg/m^3. If the merit index is doubled to $M_b = 0.006$, the upper line is valid. This line indicates that candidate materials are woods, composites, and ceramics.

A second criterion is stiffness on an absolute scale; a stiff material causes less deflection of a cantilever beam than does a flexible material. In the diagram of Figure 4, a stiffness criterion corresponds to a horizontal line. Deflection

considerations are related to rotorblade geometry and dimensions, as well as to the overall design of tower and rotor, in particular the blade deflection when the rotorblade passes the tower. A sensible deflection requires a material stiffness of 10–20 GPa; for illustration, the line for E = 15 GPa is drawn in Figure 4. Materials on or above this line satisfy the criterion, and it is seen that most woods, some composites, and some porous ceramics are excluded.

In terms of materials strength, i.e., resistance against long-time fatigue loads, and extra high loads, it is also important to consider materials fracture toughness. The toughness in relation to density is collected in a similar diagram, which can be found in Reference (3). The merit index for high fracture toughness and low density shows that candidate materials are woods and composites.

MATERIALS FOR ROTORBLADES

The combined materials performance criteria identify the candidates for rotorblades as woods and composites. Woods are potentially interesting because of their low density, but their rather low stiffness makes it difficult to limit the (elastic) deflections for very large rotorblades. Even wood materials with cellulosic fibers all aligned in the major load-bearing directions are close to the maximum performance possible for wood. Furthermore, wood is a natural material and thus environmentally attractive, but at the same time difficult to obtain in reproducible and high quality, which is a requirement for stable and economical manufacturing of rotorblades and thus economically attractive wind energy.

Partly for these reasons, composites have until now been most extensively used. Below we focus on these materials.

Fibers

The materials science basis for these composites and their potential use is the existence of strong and stiff fibers (5–10) and compliant and easily processable polymers, such as thermosets and thermoplastics (11).

The strong and stiff fibers are themselves not usable for structural purposes; their good properties can be exploited only as an important component of composites. Nonetheless, it is important to describe the fibers even if the composites are the real structural materials for rotorblades.

By far the most widely used fibers are glass fibers. In recent years carbon fibers have become of increasing interest because of the requirements presented by the ever-larger rotorblades and the decreasing price of carbon fibers. Other potentially interesting fibers are aramid, polyethylene, and cellulose, all of which have moderate mechanical properties, and low or very low densities. Key data for these fibers and their composites are collected in Table 1, and the information is discussed in the following section with a focus on glass and carbon fibers.

TABLE 1 Composite materials based on the fibers listed and a polymer matrix with properties $E_m = 3$ GPa, $\sigma_m = 100$ MPa, and $\rho_m = 1.2$ g/cm^3. The composite properties are calculated from the simple composite theory (law of mixtures); the orientation factor is 1 for aligned composites and 1/3 for random composites

	Fibers			Composites					
Type	Stiffness E_f GPa	Tensile strength σ_f MPa	Density ρ_f g/cm^3	Volume fraction V_f	Orientation θ	Stiffness E_c GPa	Tensile strength σ_c MPa	Density ρ_c g/cm^3	Merit $E_c^{1/2}/\rho_c$
Glass-E	72	3500	2.54	0.5	0°	38	1800	1.87	3.3
				0.3	Random	9.3	420	1.60	1.9
Carbon	350	4000	1.77	0.5	0°	176	2050	1.49	8.9
				0.3	Random	37	470	1.37	4.4
Aramid	120	3600	1.45	0.5	0°	61	1850	1.33	5.9
				0.3	Random	14.1	430	1.27	2.9
Polyethylene	117	2600	0.97	0.5	0°	60	1350	1.09	7.1
				0.3	Random	13.8	330	1.13	3.3
Cellulose	80	1000	1.50	0.5	0°	41	550	1.35	4.7
				0.3	Random	10.1	170	1.29	2.5

GLASS FIBERS Glass is generally composed of SiO_2, Al_2O_3, and smaller amounts of other oxides (5–7). The atoms of Si and O form a lattice with no crystallographic order, and glass fibers are therefore amorphous with isotropic properties, e.g., stiffness and thermal expansion. Glass fibers are produced in several chemical compositions, for specific purposes. The glass fiber called type E (electrical) is the most widely used for composites. Glass fibers have diameters normally in the range of 10 to 20 μm and are produced from molten glass by pulling fibers from spinnerets into bundles of hundreds to thousands of individual fibers. Their surfaces are normally coated immediately with a polymer sizing, typically a silane compound, to protect the fiber against cracks and adhered water; the sizing, which is a multicomponent compound, is also designed to improve the bonding of the glass fiber surface to the polymer matrix, typically a thermoset, and thereby enhance the properties of the composite.

Glass fibers for composites have a good combination of properties: moderate stiffness, high strength, and moderate density, as listed in Table 1.

CARBON FIBERS Carbon fibers (5–7) are composed of nearly pure carbon, which forms a crystallographic lattice with a hexagonal shape called graphite. The atoms are held together by strong covalent forces inside the hexagon plane, where the atom spacing is 1.4 Å, the bonds between the hexagon planes are weak, and the spacing is large, 3.4 Å. This crystallography means that the mechanical properties have very high values in the plane of the hexagonal planes and rather low values at right angle to the planes. This also implies a high degree of anisotropy, both in mechanical properties and in thermal expansion. The crystallographic structure and anisotropy of graphite dictates the arrangement of the hexagonal planes, such that the planes must be oriented parallel to the fiber axis in order to achieve useful properties of the fibers. In all carbon fibers there is a high degree of alignment of the graphite planes, which varies somewhat depending on the type of fiber and its production method.

The carbon fibers are produced by two different methods. The first and most widely used method starts with polyacrylonitrile (PAN) fibers. These textile fibers are oxidized, stretched, and finally heat-treated at temperatures of 1500 to 2500°C. These process steps align and couple the original C-C backbone of PAN into the graphite hexagon-planes required for the fibers. The second method starts from natural tar, which contains the graphite units in a random mixture. Various processing steps lead to the production of fibers through spinnerets, which ensure alignment of the graphite planes and thus again the required properties of the fibers. The first method achieves the necessary graphite plane alignment through coupling of C-C backbones, whereas the second method aligns pre-existing graphite planes. Both methods include rather expensive raw materials and numerous and expensive processing steps. Recent efforts (in the United States) have been initiated to find cheaper raw materials, e.g., lignin from biomass, and to develop the processing economy, e.g., by reducing the number of processing steps.

Carbon fibers for composites have an excellent combination of very high stiffness, high strength, and low density, as listed in Table 1. However, the use of carbon fibers in a hybrid combination with glass fibers has today placed focus on carbon fibers with moderate to low stiffness and relatively high failure strain, so that the carbon fibers can share the loads and deform in concert with the glass fibers of moderately high failure strain.

Matrix Materials

The polymeric composites with the above mentioned fibers have matrices of polymers, typically thermosets or thermoplastics (11). Both are rather soft and flexible (low stiffness of less than 4 GPa), and their main purpose is to bind the fibers together so that they can act in concert and give a functional composite for structural purposes. The toughness and especially failure strain is moderate for thermosets, 5–8%, and large for thermoplastics, 50–100%, and the matrices thus induce toughness in the composites, in particular via energy absorbing mechanisms related to the interface. The early composite materials for rotorblades were glass fibers combined with polyester, a material, as well as a processing method, taken from the boat industry. The easy availability of materials and processing was part of the reason for the rather fast development of rotorblades and wind energy in the early years.

The thermosets most used are polyesters, vinylesters, and epoxies. All have stiffness values of 3–4 GPa and densities of 1.1–1.3 g/cm^3 and thus match the fibers reasonably well. The thermosets go through an irreversible curing reaction, which implies a contraction giving internal stresses in the composites.

The thermoplastics for composites for rotorblades have been under development over the past 10–15 years. The properties have also rather low values: stiffness values of 1–3 GPa, and densities of 0.9–1.4 g/cm^3. The interest is centered on the potential recycling of thermoplastic polymers, and this has been investigated, although no clear procedure has been established for recycling of thermoplastic polymer composites. The thermoplastics go through a melting and solidification process during processing, which is potentially fast. The solidification also introduces a thermal contraction leading to internal stresses; these could be high because of the rather high melting point/processing temperature for thermoplastics, and better thermoplastics typically have higher melting points. The internal stresses, of whatever origin, affect the mechanical properties often detrimentally.

Composite Materials

The fibers and the matrix are combined into the composite (9, 10, 12–15). Many combinations and mixing ratios are possible, and the composite properties, most generally, are governed by the fibers, the matrix, and the interface established between these (normally) two components. Properties of fibers and matrices are, of course, important, and so are the ways in which they are arranged in the composite. The important parameters are their relative amounts, often described by the fiber volume fraction, and the spatial orientation of the fibers. As a simple illustration,

the stiffness of the composite E_c is controlled and calculated according to

$$E_c = \eta \cdot V_f \cdot E_f + V_m \cdot E_m, \quad 3.$$

where E is the stiffness (elastic modulus), V is the volume fraction, η is an orientation factor for the fibers, index f is fiber, and m is the matrix. For a perfect composite with no porosity, $V_f + V_m = 1$. The orientation factor is equal to 1 for aligned parallel fibers loaded along the fiber direction; for a randomly oriented fiber assembly in two dimensions (in a plane; often called a fiber-mat) the orientation factor is 1/3.

A range of values, listed in Table 1, illustrates the simple, basic mechanical properties of composites based on the various fibers mentioned above. The fibers are normally the dominant contributor to the composite properties, and for ease of comparison, all composite properties are calculated for a matrix of thermoset with parameters $E_m = 3$ GPa, $\sigma_m = 100$ MPa and $\rho_m = 1.2$ g/cm^3. For each composite based on a given fiber, the first line describes a composite with 50 volume% fibers, fully aligned $\eta = 1$, whereas the second line describes a composite with 30 volume% fibers arranged in a random planar mat.

In Table 1 the first column lists the typical fiber properties and the following columns list the calculated composite properties. The final column shows the elastic merit index for a cantilever beam, as discussed above. It is clear from the composite stiffness that all aligned fiber composites have rather high values, whereas nearly all random fiber composites have stiffnesses below the limit of 15 GPa (discussed above). Glass fiber composites have moderate properties and were selected in the early days because of availability and known processing technology. The other potential composites are slightly better, and only carbon fiber composites show significant improvements over the well-established glass fiber composites. This is the reason for the increasing use of carbon fiber composites in large and advanced rotorblades. The modern materials are in most cases a combination of glass fibers and carbon fibers in a hybrid construction. The hybrid aspects can be used on a macro scale, with selected parts of the rotorblade, typically the outer weight critical elements, made in carbon fiber composites, or the hybrid aspects can be on the material structure level where glass and carbon fiber are intermixed on a layer basis or perhaps even on the basis of individual fiber bundles or fibers. This hybrid concept is often a compromise between the improved performance of carbon fibers and the high cost of carbon fibers. Few rotorblades have been made completely of carbon fiber composites.

MANUFACTURING TECHNOLOGIES

During and after the energy crises in the early 1970s, many smaller companies and grass-root organizations started to build wind turbines for energy production, and shortly after, in the mid-1970s, utility companies took up the challenge and started building larger wind turbines, often with push and financial support from

the government. New manufacturing technologies were gradually developed and introduced by the blade manufacturers as the blades grew in size and in number produced (up through the 1990s), and an increasing concern about the working environment and more strict legislation pushed the technologies away from wet and open processes toward prepreg technology and closed mold infusion techniques.

Wet Hand-Lay-Up

In the early days, smaller glass fiber reinforced polyester blades were manufactured using the traditional wet hand-lay-up technique in open molds, which has been used for decades for building boats. The reinforcements were all glass fibers and mainly chopped strand mats (CSM) with random fiber orientation; in some cases woven fabrics were added to increase stiffness and strength. The upper and lower shells were adhesively bonded together to form the airfoil-shaped blade, see Figure 2. As the blades became longer (approaching 8 m), webs were inserted to support the airfoil and to take up both bending and shear loads, and a demand for higher stiffness and strength introduced a more dedicated fiber orientation with more fibers in the longitudinal direction of the blade. This was achieved either by using unidirectional woven fabrics (unbalanced fabrics with more fibers in one of the directions, normally the warp direction) or by laying down many parallel rovings in the length direction in between the CSMs. In some designs, these rovings served another purpose: they were used to form the root-end attachment as well. At the root-end the rovings were wound around steel bushes (small tubes), and continued back into the blade. The steel bushes formed the holes in what became the flange of the blade to be mounted to the hub. This principle is illustrated in Figure 5 and is known as a Hütter flange after the inventor Hütter, who used this technique for a wind turbine blade as early as the 1950s (16).

In the mid-1970s, at Tvind in Denmark, a group of pioneers built a three-bladed wind turbine with blade length of 27 m (17). The blades were manufactured from glass fiber and epoxy in a one-sided open mold. The lower side of the airfoil was laid up in a mold using a combination of CSM and rovings. A double Hütter flange,

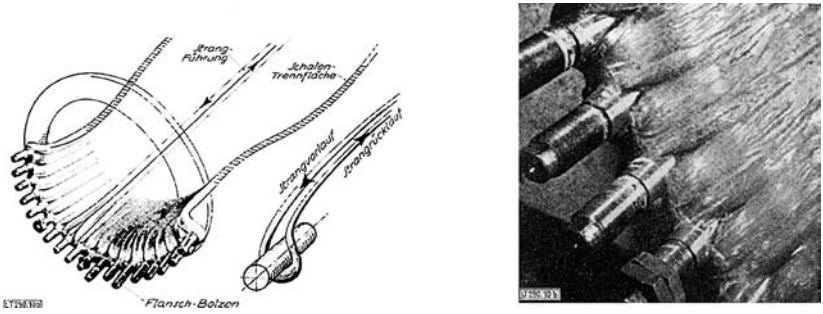

Figure 5 Principle and photo of a Hütter flange, illustrating how the fiber rovings are wound around steel bushes to form the flange (16).

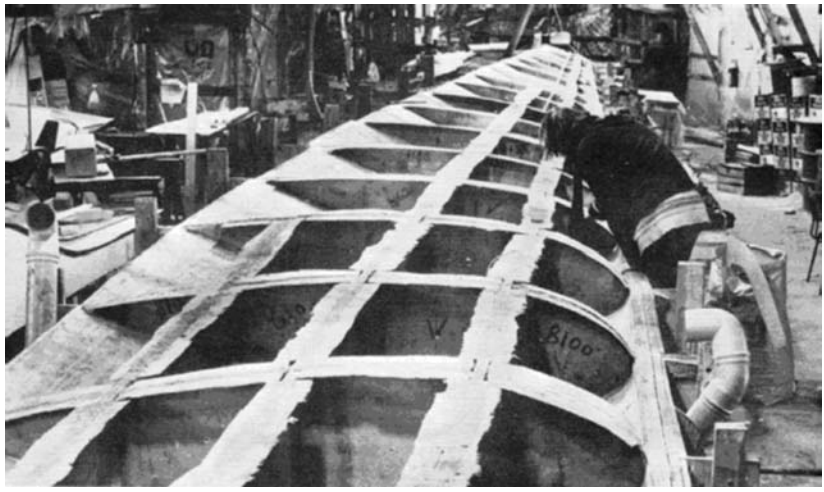

Figure 6 The Tvind blades were built in a one-sided mold. Sandwich spars and webs form the upper contour of the blade (17).

with both an external and an internal flange with bolt holes, was constructed at the same time. After curing of the lower airfoil laminate, many transverse foam spars, with the shape of the airfoil profile, were placed along the entire length of the blade at equidistant distance, and laminated onto the lower airfoil, as shown in Figure 6. Longitudinal webs were integrated, as well. The skin laminates of the webs also formed a flange toward the upper airfoil, which was built as the last part of the blade. The Tvind turbine is still in operation, but the blades were replaced in 1993 (18).

Filament Winding

When government-supported development programs for larger wind turbines started in the mid-1970s, the companies involved looked for more rational manufacturing techniques than the labor intensive hand-lay-up technique, and filament winding was investigated by several nations. Filament winding is a rational way of placing a huge amount of roving in a controlled manner around a rotating mandrel. The shape of a wind turbine blade is not cylindrical, and the majority of the fibers have to be placed along the blade length; therefore, the filament winding technique had to be developed further for this specific application.

In the United States, a technique for winding the entire blade was developed by Kaman Aerospace Corporation and Structural Composites Industries, for blades up to 45 m in length in glass fibers (19–21). A set of three mandrels was used to gradually build up the airfoil with integrated webs. First, the leading edge part and the forward shear web were wound around the first mandrel, then a second mandrel was attached to the already wound leading edge structure, and more fibers were wound onto the two combined mandrels adding more materials to the first

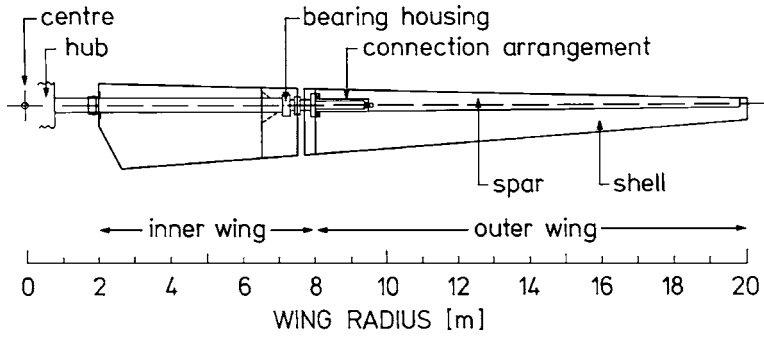

Figure 7 Principle of the Nibe blades. The inner 8 m has a steel spar and the outer 12 m is an all-composite blade (22).

structure and forming a second shear web. Finally, a third mandrel was attached, and more winding created the after body with the trailing edge. The winding was done with a combination of glass fiber roving and a glass fiber tape with most of the fibers in the transverse direction of the tape. This special tape was necessary to achieve sufficient bending stiffness and strength of the completed blade, as it is difficult and inefficient to place rovings along the axis of the mandrel with a filament-winding machine.

A tape-winding technique for winding the spar, including the leading edge and the shear web, was also developed in Denmark by Risoe National Laboratory and the Vølund company in the late 1970s (22). The blades for the two Nibe wind turbines were 20 m long and were a hybrid construction consisting of a steel spar for the inner 8 m and a glass fiber/polyester spar for the outer 12 m of the blade, Figure 7. The airfoil was hand-laid-up glass/polyester with a balsa core sandwich in the after-body, and the airfoil was adhesively bonded to the spars. Because most of the fibers must be placed along the length of the spar, a special 20-cm-wide woven glass fiber tape, with 90% of the fibers oriented transverse to the tape direction, was wound around the spar mandrel with an overlap of half the width of the tape, as illustrated in Figure 8. The thickness of the spar was easily varied along the length, from 24 mm at the root-end to 6 mm at the tip, by changing the length of travel of the tape placement apparatus along the length of the spar. Because the spar was tapered toward the tip-end and the warp glass fibers in the tape could not stretch, it was necessary to insert and withdraw a wedge underneath the tape, at the shear web position of the spar, for each revolution of the mandrel, in order to control and maintain straight fibers with the desired orientation in the upper and lower part of the spar. All the slack at the one side of the tape was taken up by the wedge, and the surplus of tape and mismatch of fiber orientation was concentrated at the web, where it actually improved the shear properties of the cured laminate. After the final layer of glass fiber tape was wound, a peel ply was applied, and the spar was parked, lined up, and cured.

Prepreg Technology

The prepreg (pre-impregnated) technology is adapted from the aerospace and aircraft industry, and it is based on the use of a semi-raw product where the fiber fabrics are pre-impregnated with resin, which is not yet cured. At room temperature the resin is like a tacky solid, and the tacky prepregs can be stacked on top of each other to build the desired laminate. By increasing the temperature, the resin becomes liquid/viscous, and the laminate can be consolidated under pressure and cured into the final component. Prepregs are available in many varieties and combinations of types of fibers, style of fabrics, and resin systems, all having different process and curing temperatures ranging from about 70 to 225°C. For large wind turbine blades, a process temperature around 80°C is most common. It results in sufficient temperature resistance of the cured laminate, and it keeps down the process and equipment costs. The required pressure to consolidate the stacked layers of prepregs is achieved by vacuum. The whole lay-up of prepreg is covered by a polymer film, which is sealed to the mold along its edge. A vacuum is pulled underneath the polymer film, and the atmospheric pressure outside the film presses the film, and thus the prepreg layers, toward the mold surface. The shelf life of the prepreg at room temperature normally ranges from days to a few weeks depending on the resin system. Therefore, the prepreg is typically stored at –18°C, resulting in a shelf life from 6 to 12 months.

The prepreg technology offers some advantages: it is easier to control and obtain constant materials properties, and a higher fiber content gives higher specific stiffness and strength of the material, which leads to lighter blades. Also, a clean process is obtained, which leads to a better working environment, with fewer requirements for the workshop ventilation systems (resulting in cost savings on smaller ventilation systems and energy needed for heating).

Vestas Wind Systems, one of the wind turbine manufacturers, uses the prepreg technology for their blade production. Vestas has used glass/epoxy prepreg technology for many years, and they have now introduced carbon fibers in their 45-m-long blades (23, 24).

Resin Infusion Technology

There are many names and variations of the resin infusion technology, which in principle consists of placing dry fibers in a mold, encapsulating and sealing off the fiber package, injecting the liquid resin into the fiber package, and curing the component. This technology was developed in the 1950s, but was used only rarely by the industry until the 1990s. Since then, the fibers, the resins, the accessories for the process, and the process equipment have been intensively developed, and resin infusion technology is now a widely used industrial process. The most important issue for the process is to ensure that all fibers are thoroughly wetted by the resin, in other words, there should be no areas with dry fibers in the final product. Most developments have concentrated on this single issue, and this problem has been tackled from many sides:

- fiber sizing with improved wettability to facilitate complete wetting without manipulating the rovings,
- fiber fabrics with special architecture to control flow pattern of the resin,
- resin with lower viscosity (at room or moderate temperature) to improve wettability and lower the process time for large components,
- resin that does not release volatiles under vacuum,
- accessories that help control resin flow pattern over large areas and ensure complete wetting of thick laminates (resin distribution mesh, special sandwich core, etc.),
- equipment for continuous mixing of resin without introducing air,
- design of molds (placement of inlet and outlet for the resin, sealing around the edge) to control resin flow to prevent entrapped area with dry fibers,
- sensors for monitoring the flow front,
- computer models for predicting and optimizing the flow pattern for a given component.

LM Glasfiber in Denmark is one of the turbine blade manufacturers that uses resin infusion technology, and it has proven to be successful in the company's most recently developed 61.5-m-long blade (25). Generally, it is normal to use a vacuum infusion technique, where all the dry fibers are covered with a polymer film sealed to the edge of the mold and held in place against the mold by a vacuum pulled underneath the polymer film, Figure 9. Thereafter, the resin line is opened, and the resin is pulled into the fiber package by the vacuum. When all the fibers are wetted, the resin line is closed, and the vacuum sucks out surplus resin into a resin trap. The atmospheric pressure outside the polymer film consolidates the laminate toward the mold surface, and the resin is allowed to cure. The two airfoils and the webs are manufactured separately, and all parts are adhesively bonded to complete the blade in a subsequent process.

Bonus Energy (now Siemens Wind Power) in Denmark has developed a special fiber placement and resin infusion technology for the company's 40-m-long blade, where the fibers for the entire blade, including airfoil, spars and webs, are placed inside a mold cavity, and the resin is infused to complete the blade in one pass (26).

The advantages of resin infusion technologies, compared with those of hand-lay-up, are the same as mentioned for the prepreg technology, except for the easy process control. As mentioned above, the challenge is to control the resin flow to avoid spots with dry fibers in the finished product.

MATERIAL MECHANICS

The mechanical behavior of composite materials is influenced by a variety of parameters. The homogeneity and quality of the materials manufactured are essential. Defects such as wrinkles, misalignment, and porosities formed during the

manufacturing process can lead to failure mechanisms such as fiber fracture, interface cracking, and matrix cracking, which are sources for microbuckling, translaminar crack growth, and delaminations. These failure mechanisms have essential influence on the resulting properties, and it is the obtainable material quality that sets the limits for the mechanical properties and their variations. From a basic materials approach the mechanical properties are controlled by the damage initiation and the damage evolution.

Damage

Talreja (27) described the mechanisms of damage in fiber, matrix, and interface in order to understand the first damage evolution in composite materials. The basic understanding of damage forms the basis for the damage continuum mechanics that has rapidly developed during the past two decades. With a focus on tension loading, Talreja (28) describes the fatigue failure mechanisms in three regions: at high loads, fiber failure; at medium loads, combined matrix and interface failure; and at low loads, matrix cracking. The damage mechanisms are different in the different regimes of the S-N curve, and accelerating the fatigue tests into another regime and extrapolating between the different regimes might lead to wrong results.

The degree of damage in a polymer matrix composite can be followed by measuring the decrease in elastic stiffness from the beginning to the end of the lifetime of the material (29). The stiffness versus number of cycles relation shows a progress that can be divided into stages (30–32). The first stage is a short initial phase with a rapid decrease in stiffness. The second stage is a steady-state phase where the rate of decrease in modulus is constant, and the third stage is a failure stage where the stiffness falls drastically because of fatal failures. Independent of damage stage, the rates of change in stiffness and the lifetime depend on the failure mode region where the material is loaded. The rates of change in stiffness of the material are defined as the damage growth rate. In order to generalize these considerations, this rate is normalized, and a linear relation between the normalized stiffness and the corresponding number of cycles is likely to be valid. Using this relation, the stiffness degradation at a given loading level for a prescribed number of cycles can be predicted. Under the assumption that the stiffness change is history independent, a model was suggested (30). On the basis of the constant amplitude S-N-curves, this model can predict the lifetime of the material when subjected to variable loading conditions, for example, stochastically defined or block-defined loading histories (31).

Recently, continuum damage mechanics have also been used to model the influence of environment, frequency and other state variables on the mechanical properties. This modeling, which is a part of the OPTIMAT (33, 34) project, was initially presented by Megnis, Brøndsted, and others (35, 36). In these papers the use of internal state variables describing the degradation of the material caused by external conditions is introduced. Each variable has an effect on the damage evolution, exemplified by the change in stiffness of the material. In its final form, it is expected that this material model can be used in the design considerations.

MECHANICAL PROPERTIES

The wind turbine blades are designed toward stiffness and fatigue. Hence, the materials required for the blades are materials with a very high performance. Their exceptionally high stiffness to weight and high strength to weight ratios, together with an excellent fatigue performance, are the reasons for composite materials being the dominant choice. Basically, the elastic properties can be calculated on the basis of the properties of the individual constituents (fiber and matrix) and the knowledge of the lay-up (i.e., fiber orientation, fiber volume fraction), Equation 3. In these cases, either the simple rule of mixture can be used or more advanced laminate calculation procedures are available. The calculations are experimentally verified by static testing measuring tension, compression, and shear properties. The demands on higher stiffness affect the fatigue behavior because materials with a higher stiffness are generally more fatigue sensitive. Consequently, the fatigue strength is approaching the performance limits, and the fatigue limits of the materials become the main limiting factor.

Stiffness, static strength, and fatigue performance are measured by testing test coupons or components. The properties measured are used to qualify the materials and to ascertain that the materials fulfill the design demands originated in the aero-elastic modeling of the blades under expected wind loads. Uniform static tests are carried out under quasistatic loading, and fatigue tests are carried out under varying loading conditions. Properties are measured under tensile loads, compressive loads, shear loads, or combinations of these in bi- and multiaxial loading modes.

During the past two decades valuable experience has been obtained in different national and international research programs. In three European projects, from 1986 to 1996 (37–39), research was focused on the mechanical behavior of the wind turbine blades and the materials. In these programs static properties, as well as the high cycle fatigue behavior of glass-polyester and glass-epoxy materials, were measured. Test techniques were developed and design curves based on constant load amplitude tests and on variable amplitude tests using stochastic load histories were established. The results from these projects were collected in two books edited by Kensche (40) and Mayer (41). De Smet & Bach collected the data into a database FACT (42).

Supported by Sandia National Laboratories, Montana State University has worked intensively since 1989 on characterizing composite materials for wind turbines. The results from this nationally supported program are collected in a large database, the DOE/MSU database, first presented in 1997 by Mandell & Samborsky (43). Since 2001 the database has been updated annually (44).

The European activities have continued in a currently running European project (2001–2006), OPTIMAT (33, 34), under the 5th EU framework program. This project aims to provide accurate design recommendations for the optimized use of materials within wind turbine rotorblades and to achieve improved reliability. The project is investigating the structural behavior of the composite material

(glass-epoxy) under the unique combination of conditions experienced by rotor-blades such as variable amplitude loading, complex multiaxial stress states (45, 46), extreme environmental conditions, thick laminates, and their possible interactions. Techniques will be developed for damage mechanics (35), life extension, condition assessment, and repair. The increasing demands for design toward stiffness and fatigue strength have required development of more accurate and reliable testing techniques.

Static Tests

TENSILE TESTING Tensile testing of composite materials (48) is performed using well-established techniques and is governed by standards, where the ASTM D3039 (49) and ISO 527 (50) are the most well documented and widely used. Making between five and ten tests on small specimens usually generates the static strength data of the materials, e.g., modulus, Poisson ratio, strength, and strain properties. The standards deal with tensile testing of both unidirectional and multidirectional fiber composites. Figure 10 shows a tensile set-up with non-contact extensometry.

COMPRESSION TESTING Compression strength is the most critical static property of many composite materials. The compression strength of unidirectional carbon fiber epoxy is about 60% of the static tensile strength. Basically, the failures in these cases come from microbuckling of the fibers, and several papers have treated this problem on a micromechanical approach (48). Fleck (51) showed in a review on the main mechanics of compressive failure that from a stability point of view the fiber alignment must be within $\pm 1^{\circ}$ in order to avoid microbuckling and instability. Figure 11 shows a kink-band formed through two porosities.

Because the main fiber direction in the flanges of the wind turbine blades is unidirectional, it has become the main topic for optimizing the manufacture of unidirectional materials. In order to document these properties, many attempts have been made to develop the most reliable test methods for documentation. Compression test of unidirectional composites is probably the most contentious type of testing. In a compression test, the critical factor appears to be from instability. This sets the requirements for the test set-up and alignment of test fixture. Early suggestions were to use supported test fixtures, such as the Celanese fixture and the IITRI test fixture (Lamothe & Nunes) (52), adopted in the ASTM D3410 (53), and the Boeing fixture defined by ASTM D695 (54), which suggested a supporting jig for thick specimens. Several other techniques of antibuckling support have been suggested, but all have given contradicting results. Adams & Welsh (55) suggested a combined loading compression test method where the load transfer to the test specimen are controlled end loading and shear loading introduced from the sides of the specimens. Also Adams (56) discussed the use of tabbed and untabbed compression specimens, but neither of these test techniques has resulted in convincing results, especially when focusing on unidirectional carbon fiber composites. In

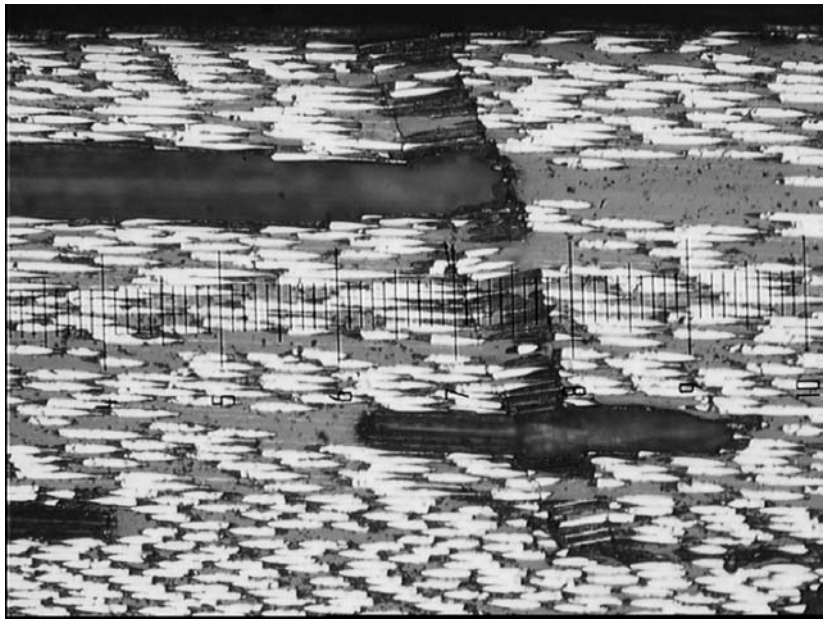

Figure 11 Microbuckling initiated in compression between two porosities. (Scale unit: 10 μm.)

1999 an ISO standard for compression testing (ISO 14126) (57) was released. This standard takes the bending during test into account and gives a maximum bending ratio for accepting the test results.

In order to further reduce the bending and to gain a closer control of the end to shear load ratio, a new concept of the combined compression test fixture was developed at Risoe National Laboratory (Figure 12).

This concept of performing compression testing appears to be very successful. Bending is almost avoided, and it has been possible to obtain compression strengths of carbon-epoxy composites that are 30–40% higher than those measured earlier. In the OPTIMAT project it has been shown that even for glass/epoxy, the compression strengths measured are 20% higher when using a combined loading fixture compared with those used testing a short-gauge-length free specimen.

SHEAR TESTING The knowledge of the shear properties of the composite is also vital when modeling structural behavior (48). The shear modulus is most successfully measured by the V-notch beam method [Iosipescu 1967 (58)] standardized in ASTM D 5379 (59). However, when measuring laminate shear properties, the $\pm 45^\circ$ tensile test can be used [ISO 14129 (60) or ASTM D 3518 (61)]. Interlaminar shear is measured by the rail shear test [ASTM D3846 (62)] or by the short beam bending test ILSS [ASTM D2344 (63)], which, however, is not suitable

for measuring design data and is mainly used in production control and data comparison.

Fatigue

On the basis of the load histories predicted for the blades, strength requirements are calculated for the materials. It must be verified that the fatigue strength for a given lifetime meets the requirements. These requirements are established by different national (64) and international recommendations, i.e., the DNV-Risoe guidelines (65) or the Germanischer Lloyd Wind Energy guidelines (66).

The results from the large research programs (33, 37–39, 42, 44) have contributed considerably to the general knowledge of the fatigue behavior of the composite materials. A variety of models have been used for describing behavior and degradation, and damage evolution in the materials has been suggested (67). Some models are constitutive ones based on physical and mechanical observations, and other models are empirical mathematical descriptions of experimental data gained. Using an extensive collection of papers and reports, Sutherland (68) published an extensive review paper on the fatigue properties of materials for wind turbines. In this review the behavior of metallic materials and woods are included.

In order to verify the models and approve the materials used to provide a given fatigue lifetime, extensive testing has focused on design considerations. Only a few standards exist for measuring the fatigue performance of the composites materials. For tension-tension fatigue, ASTM D3479 (69) gives very brief guidelines for a tensile test specimen, with an axial tension-tension cyclic loading. This standard does not prescribe clamping procedures, frequencies, or data reduction, and thus it has little value in practical applications. Late in December 2003 another international standard, ISO 13003 (70), was published defining general procedures for fatigue testing. This standard addresses all modes of testing and test machines. However, suggestions for procedures and data evaluations are still very vague and do not consider any newer findings and research results.

LOADING HISTORIES The wind speeds and the wind resources on the turbines have been extensively studied and are described in the design manuals (65, 66). On the basis of the measurements on nine different wind turbines in Europe, and representing approximately two months in service of a virtual wind turbine, a model simulating the load conditions in a blade (based on the loads in the flapwise direction measured at a point close to the blade root) has been introduced in the WISPER load sequence. WISPER (WInd SPEctrum Reference) has been used as a standardized load spectrum for horizontal axis wind turbine blades. The spectrum was developed in an IEA working group in 1987 (71). A truncated spectrum WISPERX, containing only 10% of the cycles, was later developed in order to reduce test time. The WISPERX was applied as testing sequences in the beginning of the 1990s.

However, to a considerable degree fatigue testing has been carried out as constant amplitude tests. The constant amplitude tests form the basis for understanding the fatigue damage models and are the basis for formulating models predicting the behavior under stochastic loadings. The actual loading on the blades brings the material into tension-tension fatigue and compression-compression fatigue and in some parts of the blades into tension-compression fatigue. The loading type is described by the parameter R = minimum load/maximum load. Because of the typical loads on the blades, three loading modes are normally tested. They are tension-tension fatigue (R = 0.1), tension-compression fatigue (R = −1), and compression-compression fatigue (R = 10). Most tests are performed at relatively low frequency (5–10 Hz) in order to keep down the temperature increase from hysteresis loss heating of the test specimen. In order to gain very high cycle fatigue data, Mandell et al. (72) have developed a test set-up in which they tension-tension loaded few-fiber specimens. The test equipment is based on a set-up with a loudspeaker as loading medium. At frequencies up to 200 Hz, they report data into the 10^9–10^{10} cycles regime. Although showing a large scatter, the data are consistent with extrapolated low-frequency data. From the University of Latvia, Apinis (73) has recently published a description of a high-frequency fatigue test machine based on an electrodynamic vibration exciter. Using this machine, a series of high-frequency tests on standard test coupons from the European Joule projects have been tested into the ultra-high cycle regime at 300 to 500 Hz. Results were compared with the low-frequency results reported in the FACT database (42). In that paper the authors deal with the results as if they represented a single population. However, it is our opinion that the results from high-frequency tests are grouped in two populations of which the data from the low-frequency tests show the highest performance, which indicates that a frequency effect exists. It is still not clear if viscoelastic effects and temperature effects can explain the frequency effect.

Data Handling

Making between 5 and 20 tests on small specimens usually generates the fatigue strength data of the materials. The Wöhler diagram (or S-N curve) describes the relation between the loading parameter, which can be maximum values, amplitudes, or ranges (two × amplitude) and the number of cycles to failure with a constant mean value or R-value. The Wöhler diagram is illustrated in Figure 13 using selected data from the OPTIMAT database.

A number of experimental investigations (59, 60, 74–78) on fiber-reinforced materials for rotorblades have shown that the fatigue strength, S, at a constant R-ratio can be described by the analytical relation suggested by Basquin in 1910.

$$N_f \cdot S^m = C, \qquad 4.$$

where C is a constant, N_f is the number of cycles to failure, and m is a shape parameter (Wöhler exponent) reflecting the slope of the log-log line in the Wöhler

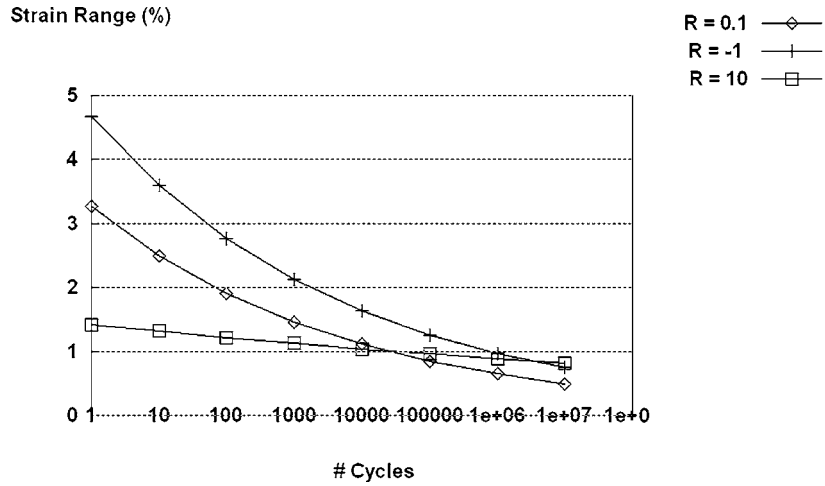

Figure 13 Wöhler diagram showing 50% regression lines based on data from the OPTMAT database.

diagram. A high m-value (>10) reflects a flat curve and a moderate m-value (1–10) reflects a steeper line. (The fatigue strength, S, can be either on a strain, stress or load basis.) Continuous fiber-reinforced polymers cannot be assumed to have a fatigue limit but will continue to degrade according to the equation above.

Alternatively, as mentioned by Sutherland, the S-N presentation can be fitted using an exponential function

$$N \cdot 10^{m_1 S} = C_1, \qquad 5.$$

which results in a straight line relationship in a log-linear diagram. This empirical model has mainly been applied to present the data from the DOE/MSU database (43, 44).

However, the dependent parameter N is a two-parameter function depending on both the applied amplitude and the applied mean value. The third dimension in the fatigue parameter space can be illustrated in the Haigh (or Goodman) diagrams (79). These diagrams can be plotted showing the relationship between mean value and amplitude or range at a particular fatigue life. This is illustrated in Figure 14. A point in this type of diagram represents a given number of cycles to failure, i.e., one point marks at which range and mean level the lifetime will be the preset number of cycles. Straight lines through the origo in this diagram show "iso-R" lines and test results from tests run at constant R-values lie on these lines. If the test results are positioned on vertical lines, it means that the tests were run at constant mean values. Combining the Haigh diagram and the Wöhler diagram gives a three-dimensional plotting of the fatigue results, as shown in Figure 15. The relationships between mean and amplitude or range for metals were suggested by Goodman (80) and Gerber (81) in the 19th century, long before the synthetic

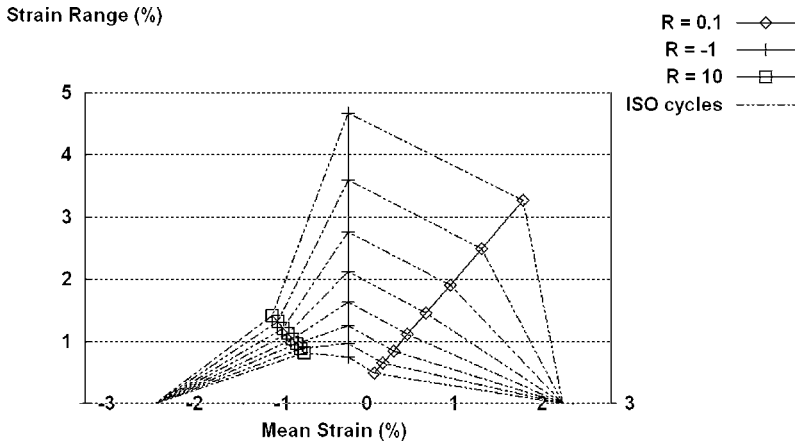

Figure 14 Haigh diagram based on the fitted data in Figure 13.

polymers were invented and nearly a century before continuous fiber composites were introduced. The Gerber and Goodman relationships can be formulated in the following expression:

$$S_a = S_c \cdot \left(1 - \frac{S_m}{S_u}\right)^c, \qquad 6.$$

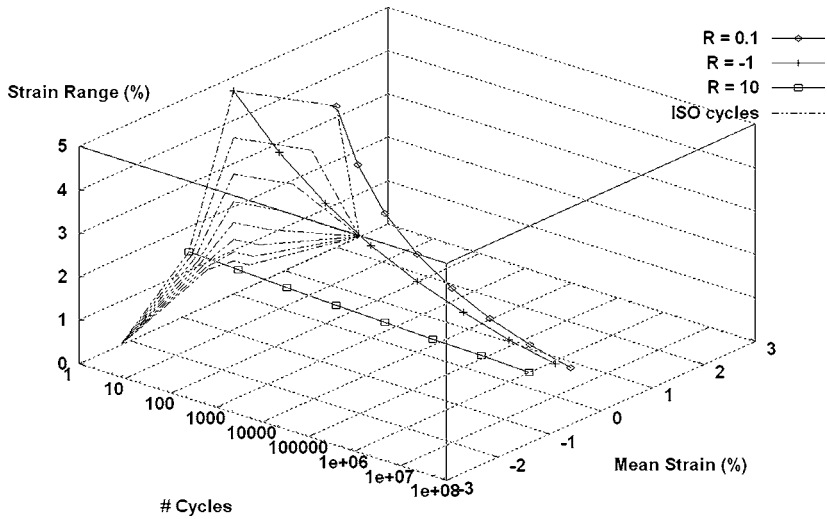

Figure 15 Combining Figure 13 and Figure 14 gives a three-dimensional illustration of the relationship between Haigh diagrams and Wöhler diagrams.

where S_a and S_m are the amplitude and mean values, respectively, S_c is the fatigue limit, and S_u is the ultimate value of the strength parameter, and c is a constant equal to 1 for the Goodman relationship and equal to 2 for the Gerber suggestion.

Sutherland (67, 68) has reported several efforts to plot data mainly from the DOE/MSU database into Haigh diagrams. An attempt has been made to use Gerber or Goodman relationships, but for composites no empirical or analytical relationship between mean values and amplitudes at fixed numbers of cycles could be established.

It is advantageous to be able to compare variable amplitude (VA) fatigue test results to constant amplitude (CA) fatigue test results in order to present them on a simple parametric form.

Palmgren (82) and Miner (83) suggested that cumulative damage in fatigue during a VA test can be reflected in one parameter, the Palmgren-Miner sum, calculated as

$$\mathrm{M} = \sum_{\mathrm{i}=1}^{\mathrm{j}} \frac{\mathrm{n_i}}{\mathrm{N_i}}, \qquad 7.$$

where i is the level number in the VA test, $\mathrm{n_i}$ is the number of cycles at level i in the VA test, $\mathrm{N_i}$ is the cycles to failure in the CA test at level i, and j is the number of different load levels. This sum forms the basis for the Palmgren-Miner rule, which states that failure takes place when M equals 1. This relationship is based on fatigue of metals, and for this group of materials the exponent m of the S-N curve is of the order of 3. The S-N line for metals is much steeper than the S-N lines for glass and carbon fiber composites where the exponent m is 10–25.

A method of predicting VA lifetimes based on CA findings was suggested by Dover (83a) and descriptions of methods for comparing fatigue lives for spectrum loading was reported by Solin (83b), which together have been successfully used in evaluating stochastic load data on steel structures. The most successful methods are based on the calculation of an equivalent loading value. An equivalent fatigue stress or strain, $\mathrm{S_{eq}}$, of a VA fatigue test is defined as the CA fatigue level at which failure takes place after the same number of cyclic loadings. Brøndsted et al. adapted this concept (84) for analyzing fatigue tests using block loading and WISPERX spectrum loading.

Combining the Basquin equation and Palmgren-Miner rule with $\mathrm{n_i}$ as the number of cycles at different load levels, $\mathrm{S_i}$, the equivalent stress or strain, $\mathrm{S_{eq}}$, is calculated from

$$\mathrm{S_{eq}} = \mathrm{C}^{\frac{1}{\mathrm{m}}} \cdot \left(\sum \mathrm{n_i} \right)^{-\frac{1}{\mathrm{m}}}, \qquad 8.$$

and an expression for the normalized equivalent stress is given as

$$\mathrm{S_{eq}} = \left(\frac{\sum (\mathrm{n_i} \cdot \mathrm{S_i^m})}{\sum \mathrm{n_i}} \right)^{\frac{1}{\mathrm{m}}} \cdot \left(\frac{1}{\mathrm{M}} \right)^{\frac{1}{\mathrm{m}}}. \qquad 9.$$

M is the Miner sum. It is seen that the equivalent stress value depends on $M^{\frac{1}{m}}$. Knowing the Palmgren-Miner sum, VA fatigue lifetimes can now be predicted based on the CA fatigue test results and the knowledge of the variable load history.

Hence, a comparison between CA test results and VA test results is possible by assuming that $M^{\frac{1}{m}} = 1$, but the validity of the Palmgren-Miner rule, $M = 1$, can be discussed. A typical m-value of metallic materials is 3. Allowing S_{eq} to vary within values of 10% means that $M^{\frac{1}{m}}$ can vary between 0.9 and 1.1. Now taking the power into account, this means that an acceptable variation in M is in the range from 0.73 to 1.33. For glass fiber polymer composites the exponent m is of the order of 10, and the acceptable variation in M ranges from 0.3 to 2.6. Furthermore, for carbon fiber composites, ceramics, and other very brittle materials the exponent m is found to be up to 20 or 25, which leads to a very large acceptable variation in the Miner sum. Therefore, using the Palmgren-Miner sum when comparing VA and CA fatigue test results, the slope of the constant amplitude S-N curve is a key parameter. The Miner sum M is hereby shown to be too dependent on the slope m and is therefore not a suitable parameter to use because high exponent (m) values give a large scatter in the Miner sum (M).

By testing this rule it has been found that failure can take place in cases where the sum is significantly lower than 1 (unsafe as a design rule) and where it is considerably higher than 1 (safe as a design rule); therefore, lifetime predictions alone cannot be based on this rule. A large scatter in the Palmgren-Miner sum is often explained by the degree of sequence dependence, which can be beneficial ($M > 1$) or detrimental ($M < 1$).

Environmental conditions, which affect the materials fatigue behavior, should be considered and taken into account. Such conditions in particular include humidity and temperature, both of which may lead to degradation of strength and stiffness. Their design effects calculated by introducing appropriate partial coefficients as safety factors should be applied in the strength analysis. Not much has been published thus far on environmental effects, but such investigation is a part of the OPTIMAT project.

STATISTICAL DATA ANALYSIS

The S-N curve is often analyzed by linear regression analysis of the S-N data pairs in log-log or in log-linear mode depending on the expression adopted. However, because the statistical distribution is unknown, the ASTM E739 (85) does not recommend either extrapolating the lines outside the interval tested or using the common practice of introducing a 95% confidence line as a design line. Furthermore, it cannot be recommended to use another common practice, which is to define the upper design bounds by subtracting two or three times the standard deviation. Because the design lifetime of a wind turbine blade goes into the very high cycle range, one could either adopt dubious accelerated high cycle fatigue test data or turn to conservative statistically calculated upper bounds for the design

lines. A statistical method for predicting lifetime was suggested by Echtermeyer et al. (86), and Ronold & Echtermeyer (87) presented the theoretical basis. They showed the possibilities for establishing characteristic values for unconditioned and conditioned variables and introduced a mathematical concept of calculating 95% tolerance bounds with a 95% confidence interval.

CHALLENGES

Thermoplastic Composites

Since the 1980s different types of thermoplastic composites with continuous fibers have been on the market, ranging from carbon fiber/PEEK to glass fiber/PP. The drive for using thermoplastic composites is higher toughness, faster processing, unlimited shelf life of the semi-raw materials, a clean working environment, and potential for much easier recycling of the material. Factors that have held back the thermoplastic composites from being used for wind turbine blades are high process temperature (requires high temperature resistant tooling and accessories), introduction of new process technologies, and more difficult adhesive joining.

In principle, the manufacturing technology for traditional thermoplastic composites is simple. It consists of (*a*) heating the material to melt the thermoplastic polymer, (*b*) consolidating the material under pressure to form the composite material and the component, and (*c*) cooling the material to return the polymer to a solid state. For those thermoplastic matrix materials that can be used continuously at elevated temperatures, such as 80–250°C, the processing temperature is in the range of 180–390°C, and special care is required in designing tools and selecting accessories regarding thermal expansion and thermal resistance (88).

Recently, a new type of cyclic thermoplastic polybutylene terephthalate (PBT) resin has been developed. It has a very low viscosity at the processing temperature and is suitable for the resin infusion technology (89). At the process temperature, which is around 180°C, a reaction transforms the liquid polymer into a solid thermoplastic polymer.

Several wind turbine blade manufacturers have been or are involved in programs where the use of thermoplastic composites for blades has been or is being investigated. In 1996, LM Glasfiber, Comfil, and Risoe National Laboratory developed a concept for manufacturing airfoils for blades in glass fiber/L-PET (a modified PET with process temperature of 220°C) (88, 90, 91). The concept was demonstrated on a 3.2-m-long airfoil. In 1999 Bonus Energy and Risoe National Laboratory developed a concept for manufacturing complete blades in one pass in a glass fiber/PP composite material at a process temperature of 180°C. That concept was demonstrated on a short blade section of 0.5 m, as illustrated in Figure 16 (92). In 2004, Gaoth Tec, Cyclics, and Mitsubishi initiated a development program for a 12.6-m-long blade manufactured by a resin infusion technology using a thermoplastic resin from Cyclics (93).

Structural Materials

New materials and materials concepts are illustrated in Table 1, where the fibers of polymer origin have potential, in particular due to their low density. The merit index $E^{1/2}/\rho$ is more affected by (reduced) density than (increased) stiffness, so (very) light materials are of particular interest for weight critical components such as large rotorblades. At present none of the composites based on aramid, polyethylene, or cellulose fibers has been developed to an industrial technical level, which could make them practically interesting for large rotorblades. Two of the polymer fibers, aramid and polyethylene, are based on crude oil, i.e., a non-renewable resource, whereas the cellulose fibers are based on biomass, which is a renewable resource. The increasing focus on environment and ecology, as well as on limited resources, may make the cellulose fibers particularly interesting for demanding structural applications, such as large rotorblades.

New Structural Design

An important goal for rotorblade manufacturers is the reduction of blade weight relative to the length. This is both structurally necessary, as discussed above, and economically attractive because it will lower the cost of rotorblades and thus eventually reduce the cost per energy unit produced (cost/kWh). In addition to the new materials concept, the structural design has also been improved over the years. The three new data points in Figure 3 show the weight reduction achieved for essentially glass fiber composite blades, by improved design ideas (as well as some use of carbon fiber composites). The structural design of the heavy root section of rotorblades has been optimized (although details are not available), leading to thinner root diameters for longer blades and thus smaller, lighter, and less expensive hubs.

The special behavior of anisotropic non-symmetrical laminates under combined bending and twisting has been exploited to design composite laminates and blade structures where the blade bends and twists simultaneously under heavy loads. Thus the aerodynamic profile of the rotorblade can be made to adjust itself optimally at low wind speeds for maximum aerodynamic performance, and to twist itself out of the wind at high wind speeds so that the loads on the blade are reduced. An additional advantage under heavy winds is that the normal pitch control, which physically rotates the blades around the blade axis, is slow to respond to gusts, so here the active blade twisting helps in controlling the blade and rotor performance under the always varying wind conditions, i.e., wind speed and wind direction.

New Structural Health

With still larger rotorblades and the associated risks, and with the constant striving to improving the economy of wind energy, the rotorblades need to be designed

both safely and to the limit, to avoid over-design and over-weight. In this context, materials research needs to better understand the continuous degradation of fiber composites under (long-time) fatigue loading and to develop models for prediction of lifetimes.

Structural health monitoring has been under development recently to allow continuous recording of important parameters for the state of degradation/damage of the materials. The state of degradation is a measure of the remaining lifetime and when reliable models exist accurate prediction of lifetime can be made. Any extraordinary change in the state of degradation can be used to initiate inspection, repair, or replacement of rotorblades. Recently, large rotorblades have been fitted with monitoring systems having embedded optical fibers and related software, which record loads, temperature, damage, and lightning strikes (25).

Trends and Markets

The trends for rotorblades are for increasing size and, most critical, reduced weight. This couples with the ever-increasing size of turbines, which are supposed to deliver reduced costs for wind energy (cost/kWh). The materials and, in particular, composites are important elements in this development because they deliver low density, good stiffness, and potentially long lifetimes. New trends in the materials occur with respect to properties, design, and monitoring, as well as manufacturing technology. Today's markets are world wide, with suppliers of wind turbines mainly located in Europe (72%), with activities in United States (18%) and Asia (10%) (1). The wind turbines are generally being placed off-shore in parks or farms, both to exploit the more free and generally stronger winds and also to reduce the environmental effects on land.

In order to meet the challenge as wind turbine blades grow longer and to allow for the next generation of larger wind turbines with intelligent blades, higher demands are placed on materials and structures. This requires more thorough knowledge of materials and safety factors, as well as further investigation into new materials. Furthermore, a change in the whole concept of structural safety of the blade is required. Kensche (94) reviewed the trends in the fatigue investigations of materials for wind turbines. He points out that many topics remain to be explored. In particular, there should be a focus on the basic understanding of damage and failure mechanism, effects and interpretation of the stochastic loadings, multiple stress states, environmental effects, size effects, and thickness effects. New initiatives are in progress in the field of condition monitoring (structural health monitoring), and several manufacturers of wind turbine blades are already fitting the blades with sensors. The challenge is to be better able to interpret the signals and to know the actions to take. This requires an even better basic understanding of the life cycle behavior and the degradation mechanisms.

The *Annual Review of Materials Research* is online at http://matsci.annualreviews.org

LITERATURE CITED

1. BTM Consult ApS, World Market Update 2003—March 2004. 90 pp.
2. NewsLetter, May 2004. LM Glasfiber A/S. www.lm.dk
3. Ashby MF. 1992. *Materials Selection in Mechanical Design*. Oxford, UK: Pergamon. 312 pp.
4. Lovatt A, Shercliff H. 2002. Material selection and processing. http://www-materials.eng.cam.ac.uk/mpsite/interactive_charts/
5. Watt W, Perov PV. 1985. Strong fibres. In *Handbook of Composites*, ed. A Kelly, YN Rabotnov. Amsterdam: North-Holland/Elsevier. 755 pp.
6. Bunsell AR. 1988. *Fibre Reinforcements for Composite Materials*. Amsterdam: Elsevier. 537 pp.
7. Chou TW, ed. 2000. Fibre reinforcements and general theory of composites. See Ref. 95, 1:802
8. Lilholt H, Lawther JM. 2000. Natural organic fibers. See Ref. 95, 1:303–325
9. Lilholt H, Toftegaard H, Thomsen AB, Schmidt AS. 1999. Natural composites based on cellulose fibres and polypropylene matrix. *Proc. Int. Conf. Compos. Mater.,12th, Paris, Pap. 1115*. 9 pp.
10. Lilholt H, Madsen B, Toftegaard H, Cendre E, Megnis M, et al., eds. 2002. Sustainable natural and polymeric composites—science and technology. *Proc. 22nd Risoe Int. Symp. Mater. Sci. Risoe Natl. Lab., Roskilde, Denmark.* 371 pp.
11. Talreja R, Månson J-AE. 2000. Polymer matrix composites. See Ref. 95, 2:1129
12. Jones RM. 1975. *Mechanics of Composite Materials*. New York: McGraw-Hill. 355 pp.
13. Hancox NL, Mayer RM. 1994. *Design Data for Reinforced Plastics, A Guide for Engineers and Designers*. London: Chapman & Hall. 326 pp.
14. Lilholt H, Talreja R, eds. 1982. Fatigue and creep of composite materials. *Proc. 3rd Risoe Int. Symp. Metall. Mater. Sci. Risoe Natl. Lab., Roskilde, Denmark.* 341 pp.
15. Andersen SI, Brøndsted P, Lilholt H, Lystrup Aa, Rheinlaender JT, et al., eds. 1997. Polymeric composites—expanding the limits. *Proc. 18th Risoe Int. Symp. Mater. Sci. Risoe Natl. Lab., Roskilde, Denmark.* 525 pp.
16. Hütter U. 1960. Tragende Flugzeugteile aus glasfaserverstärkten Kunststoffen. *Luftfahrttechnik* 6:2:34–44
17. Tvindskolerne. 1977. Lad 100 møller blomstre. 6 ed. *Forlaget Skipper Klement. Special-Trykkeriet A/S. Viborg, Denmark* (In Danish)
18. Fakta om Vindenergi. 2003. *Faktablad M5*. Danish Wind Turbine Owners' Assoc. http://www.dkvind.dk/fakta/fakta_pdf/M5.pdf. (In Danish)
19. 1976. Design study of wind turbines 50 kW to 3000 kW for electric utility application. *Kaman Rep. No. R-1382, ERDA/NASA—19404—76/2*. pp. 4–5, 4–51, 4–79. Kaman Aerospace Corp., Bloomfield, CT
20. White ML, Weigel WD. 1979. A low cost composite blade for a 300 foot diameter wind turbine. *34th Annu. Tech. Conf., Reinforced Plastics/Compos. Inst.*, Sec. 15-C: 1–6. Soc. Plastic Ind., Washington, DC
21. Weingart O. 1979. Fabrication of large composite spars and blades. See Ref. 20, Sec. 15-B:1–4
22. Johansen BS, Lilholt H, Lystrup Aa. 1980. Wingblades of glass fibre reinforced polyester for a 630kW wind turbine—design, fabrication and materials testing.

In *Advances in Composite Materials,* 2:1355–67. Oxford, UK: Pergamon
23. http://www.vestas.com/produkter/pdf/updates_020804/V90_3_UK.pdf
24. Griffin DA. 2004. Growing opportunities and challenges in wind turbine blade manufacturing. *High-Performance Composites*. http://www.compositesworld.com/hpc/issues/204/May/450
25. http://www.lm.dk
26. Griffin DA. 2004. Cost and performance tradeoffs for carbon fibres in wind turbine blades. *SAMPE J*. June/July, pp. 20–28
27. Talreja R. 1982. Damage models for fatigue of composite materials. See Ref. 14, pp. 137–53
28. Talreja R. 2000. Fatigue of polymer matrix composites. See Ref. 95, 2:529–52
29. Stinchcomb WW, Bakis CE. 1990. Fatigue behavior of composite laminates. *Fatigue of Composite Materials*, ed. KL Riefsnider, pp. 105–80. Amsterdam: Elsevier
30. Andersen SI, Brøndsted P, Lilholt H. 1996. Fatigue of polymeric composites for wingblades and the establishment of stiffness-controlled fatigue diagrams. *1996 Eur. Union Wind Energy Conf. EWEC '96, Göteborg*, pp. 954–59. Bedford: HS Stephens & Assoc.
31. Brøndsted P, Lilholt H, Andersen SI. 1997. Fatigue damage prediction by measurements of the stiffness degradation in polymer matrix composites. In *Int. Conf. Fatigue Compos.,1st, Paris, 8. International spring meeting of ICFC, Paris*, pp. 370–77. Paris: ICFC
32. Brøndsted P, Johansen BS. 1999. Measurement of damage progress in FRP materials. *Plast. Rubber Compos.* 28:9:458–62
33. EU FP5. 2001–2006. Reliable optimal use of materials for wind turbine rotor blades (OPTIMAT BLADES). ENK6-CT-2001-00552. http://www.wmc.tudelft.nl/optimat_blades/
34. van Wingerde AM, Nijssen RPL, van Delft DRV, Janssen LGJ, Brøndsted P, et al. 2003. Introduction to the OPTIMAT BLADES project. In *Proc. CD-ROM CD 2, Eur. Wind Energy Conf. Exhib. 2003*, *Madrid, Spain, 16–19 June*, p. 9. Brussels: Eur. Wind Energy Assoc.
35. Megnis M, Brøndsted P, Rehman SA, Ahmad T. 2004. Life predictions of long fiber composites in extreme environmental conditions using damage evolution approach. *Proc. 11th Eur. Conf. Compos. Mater., Rhodes, Greece*, 10 pp. London: Eur. Soc. Compos. Mater.
36. Megnis M, Brøndsted P, Rehman SA, Ahmad T. 2004. Characterization of internal state variable for fiber fracture in UD composite. *Int. Conf. Advances in Computational and Experimental Engineering and Sciences, Madeira, Port*, pp. 451–56. Encino, CA: Tech Science Press
37. 1987–1989. EC Proj. No. EN3W.0024. *Design basis for wind turbines*.
38. EC-JOULE-1 programme. 1990–1993. *Fatigue Properties and Design of Wingblades for Windturbines.* Contract no. JOUR-0071-DK (MB)
39. EC-JOULE-2 programme. 1992–1995. *Development of Advanced Blades for Integration into Wind Turbine Systems.* Contract no. JOU2-CT92-085
40. Kensche CW, ed. 1996. *Fatigue of Materials and Components for Wind Turbine Rotor Blades*, *EUR 16684.* Eur. Comm., Luxembourg
41. Mayer RM, ed. 1996. *Design of Composite Structures against Fatigue. Mechanical Engineering*. Suffolk, UK: Publications
42. De Smet BJ, Bach PW. 1994. Database FACT: Fatigue of composites for wind turbines. *3rd IEA Symp. Wind Turbine Fatigue*, *ECN, Petten, The Netherlands, April 22–23*
43. Mandell JF, Samborsky DD. 1997. *DOE/MSU Composite Materials Fatigue Database. Test Methods, Materials, and Analysis,* SAND97-3002, UC-1210, Sandia Natl. Lab., Albuquerque, NM

44. Update: *DOE / MSU Composite Material Fatigue Database.* February 24, 2004. http://www.sandia.gov/Renewable_Energy/wind_energy/other/973002upd0204.pdf
45. Smits A, van Hemelrijck D, Philippidis T. 2004. The digital image correlation technique as full field strain technique on bi-axial loaded composites using cruciform specimens. *ICEM12. 12th Int. Conf. Exp. Mech., Politecnico di Bari, Italy.* 8 pp.
46. Smits A, van Hemelrijck D, Philippidis T, van Wingerde AM, Cardon A. 2004. Optimisation of a cruciform test specimen for bi-axial loading of fibre reinforced material systems. *Proc. 11th Eur. Conf. Compos. Mater., Rhodes, Greece*. London: Eur. Soc. Compos. Mater. 9 pp.
47. Deleted in proof
48. Adams DF. 2000. Test methods for mechanical properties. See Ref. 95, 5:113–48
49. ASTM D3039–00. 2000. *Standard Test for Tensile Properties of Polymer Matrix Composite Materials*. W. Conshohocken, PA: Am. Soc. Test. Mater.
50. ISO 527. Plastics—Determination of tensile properties. Geneva: ISO
51. Fleck NA. 1997. Compressive failure in fibre composites. In *Advances in Applied Mechanics*, ed. JW Hutchinson, TY Wu, 33:43–117. New York: Academic
52. Lamothe RM, Nunes J. 1983. Evaluation of fixturing for compression testing of metal matrix and polymer/expoxy composites. *Compression Testing of Homogeneous Materials and Composites. ASTM STP 808*, ed. R Chait, R Papino, pp. 241–53. W. Conshohocken, PA: Am. Soc. Test. Mater.
53. ASTM D 3410–95. 1995. *Standard Test Method for Compressive Properties of Polymer Matrix Composite Materials with Unsupported Gage Section by Shear Loading*. W. Conshohocken, PA: Am. Soc. Test. Mater.
54. ASTM D695-02a. 2002. *Standard Test Method for Compressive Properties of Rigid Plastics*. W. Conshohocken, PA: Am. Soc. Test. Mater.
55. Adams DF, Welsh JS. 1997. The Wyoming combined loading compression (CLC) test method. *J. Compos. Technol. Res.* 19:3:123–33
56. Adams DF. 2002. Tabbed versus untabbed compression specimens. *Composite Materials: Testing, Design, and Acceptance Criteria, ASTM STP 1416*, ed. AT Nettles, A Zureick, pp. 1–14. W. Conshohocken, PA: Am. Soc. Test. Mater.
57. ISO 14126. 1999. *Fibre-Reinforced Plastic Composites—Determination of the Compression Properties in the In-Plane Direction*. Geneva: ISO
58. Iosipescu N. 1967. New accurate procedure for single shear testing of metals. *J. Mater.* 2(3):537–66
59. ASTM Standard D 5379. 1998. *Standard Test Method for Shear Properties of Composite Materials by the V-notched Beam*. W. Conshohocken, PA: Am. Soc. Test. Mater.
60. ISO 14129. 1998. *Fibre-reinforced Plastic Composites—Determination of the In-Plane Shear Stress/Shear Strain Response, Including the In-Plane Shear-Modulus, by the $\pm 45^\circ$ Tension Test Method*. Geneva: ISO
61. ASTM D3518. 2001. *Standard Test Method for In-Plane Shear Response of Polymer Matrix Composite Materials by Tensile Test of a $\pm 45^\circ$ Laminate*. W. Conshohocken, PA: Am. Soc. Test. Mater.
62. ASTM D3846. 1994. *Standard Test Method for In-Plane Shear Strength of Reinforced Plastics*. W. Conshohocken, PA: Am. Soc. Test. Mater.
63. ASTM D2344. 1995. *Standard Test Method for Apparent Interlaminar Shear Strength of Parallel Fiber Composites by Short-Beam Method*. W. Conshohocken, PA: Am. Soc. Test. Mater.
64. Vestergaard B, Wedel-Heinen J, Halling KM, Sønderby O, et al. 2002. In *Type Approval Scheme for Wind Turbines. Recommendation for Design*

Documentation and Test of Wind Turbine Blades, ed. C Skamris. Copenhagen: Danish Energy Agency. http://www.dawt.dk/Common/RecomBlades.pdf

65. *Guidelines for Design of Wind Turbines*. 2001. Det Norske Veritas, Copenhagen, and Risoe Natl. Lab., Roskilde, Denmark. 261 pp.
66. *Guideline for Certification of Wind Turbines*. 2003. Hamburg, Ger.: Lloyd WindEnergie
67. Sutherland HJ. 1999. *On the Fatigue Analysis of Wind Turbines. SAND99-0099*. Albuquerque, NM: Sandia Natl. Lab.
68. Sutherland HJ. 2000. A summary of the fatigue properties of wind turbine materials. *Wind Energy* 3:1–34
69. ASTM D3479. 2002. *Standard Test Method for Tension-Tension Fatigue of Polymer Matrix Composite Materials*. W. Conshohocken, PA: Am. Soc. Test. Mater.
70. ISO 13003. 2003. *Fibre-Reinforced Plastics—Determination of Fatigue Properties Under Cyclic Loading Conditions*. Geneva: ISO
71. TenHave AA. 1991. *WISPER and WISPERX Final Definition of Two Standardised Fatigue Loading Sequences for Wind Turbine Blades*. NLR Rep. NLR TP 91476
72. Mandell JF, Samborsky DD, Wang L, Wahl NK. 2003. New fatigue data for wind turbine blade materials. *J. Solar Energy Eng. Trans. ASME* 125:506–14
73. Apinis R. 2004. Acceleration of fatigue tests of polymer composite materials by using high-frequency loadings. *Mech. Compos. Mater*. 40:2
74. Brøndsted P, Andersen SI, Lilholt H. 1996. Fatigue performance of glass/polyester laminates and the monitoring of material degradation. *Mech. Compos. Mater.* 32:21–29
75. Deleted in proof
76. Echtermeyer AT, Kensche C, Bach P, Poppen CM, Lilholt H, et al. 1996. Method to predict fatigue lifetime of GRP wind turbine blades and comparison with experiments. *1996 Eur. Union Wind Energy Conf. EWEC '96, Göteborg,* pp. 907–13. Bedford: HS Stephens & Assoc.
77. Andersen SI, Brøndsted P, Lilholt H, Lystrup Aa. 1996. Risoe investigations of GI-UP materials. See Ref. 40, pp. 71–119
78. Brøndsted P, Lilholt H. 1998. *Vingedesign EFP-95 Slutrapport for Materialer*. Risoe-R-1040(DA). (In Danish)
79. Frost NE, Marsh KJ, Pook LP. 1974. *Metal Fatigue*. Oxford, UK: Clarendon
80. Goodman J. 1899. *Mechanics Applied to Engineering*. London: Longman, Green, & Co.
81. Gerber WZ. 1874. *Bayer. Archit. Ing.* 6: 101
82. Palmgren A. 1924. Die Lebensdauer von Kugellagern. *Z. Ver. Dtsch. Ingenieuren* 68:14:339–41
83. Miner MA. 1945. Cumulative damage in fatigue. *J. Appl. Mech.* 12:A159–64

83a. Dover WD. 1979. Variable amplitude fatigue of welded structures. In *Fracture Mechanics: Current Status, Future Prospects*, ed. RA Smith, pp. 129–47. Toronto: Pergamon

83b. Solin J. 1990. Methods for comparing fatigue lives for spectrum loading. *Int. J. Fatigue* 12:1:35–42

84. Brøndsted P, Andersen SI, Lilholt H. 1997. Fatigue damage accumulation and lifetime prediction of GFRP materials under block loading and stochastic loading. See Ref. 15, pp. 269–78
85. ASTM E739. 1998. *Standard Practice for Statistical Analysis of Linear or Linearized Stress-Life (S-N) and Strain-Life (e-N) Fatigue Data*. W. Conshohocken, PA: Am. Soc. Test. Mater.
86. Echtermeyer AA, Hayman B, Ronold KO. 1996. Comparison of fatigue curves for glass composite laminates. See Ref. 41, Ch. 14
87. Ronold KO, Echtermeyer AT. 1996. Estimation of fatigue curves for design of composite laminates. *Composite A* 27: 6:485–91

88. Lystrup Aa. 1997. Processing technology for advanced fibre composites with thermoplastic matrices. See Ref. 15, pp. 69–80
89. http://www.cyclics.com
90. Lystrup Aa. 1998. Hybrid yarns for thermoplastic fibre composites. *Final Rep. MUP2 Framework Program. Risoe-R-1034(EN)*. Roskilde, Denmark: Risoe Natl. Lab.
91. http://www.comfil.biz/rapport/takwind.htm
92. 1999. *Mater. Res. Dep. Annu. Rep*. Risoe-R-1155(EN). Roskilde, Denmark: Risoe Natl. Lab., April 2000. http://www.risoe.dk/rispubl/AFM/afmpdf/ris-r-1155.pdf
93. http://www.gaoth-tec.com
94. Kensche CW. 2004. Fatigue of composites for wind turbines. *3rd Int. Conf. Fatigue Composites, Kyoto, Japan*
95. Kelly A, Zweben C, eds. 2000. *Comprehensive Composite Materials*, Vols. 1–6. Amsterdam: Elsevier/Pergamon

Figure 1 The world's largest wind turbine (summer 2004) at Risoe National Laboratory test site, Høvsøre, Denmark. Tower height is 120 m, rotor diameter is 110 m, and generator power is 3.6 MW.

Figure 8 Tape winding of a spar for the Nibe wind turbines. The thickness of the spar was varied along the length, by varying the length of travel of the tape placement apparatus along the length of the spar. A wedge was manually inserted and withdrawn underneath the tape, at the shear web position of the spar, for each revolution of the mandrel, in order to control and maintain straight fibers with the desired orientation in the upper and lower part of the spar.

Figure 9 Set-up for resin infusion test of a root-end section of a large rotorblade at LM Glasfiber, Lunderskov, Denmark (25).

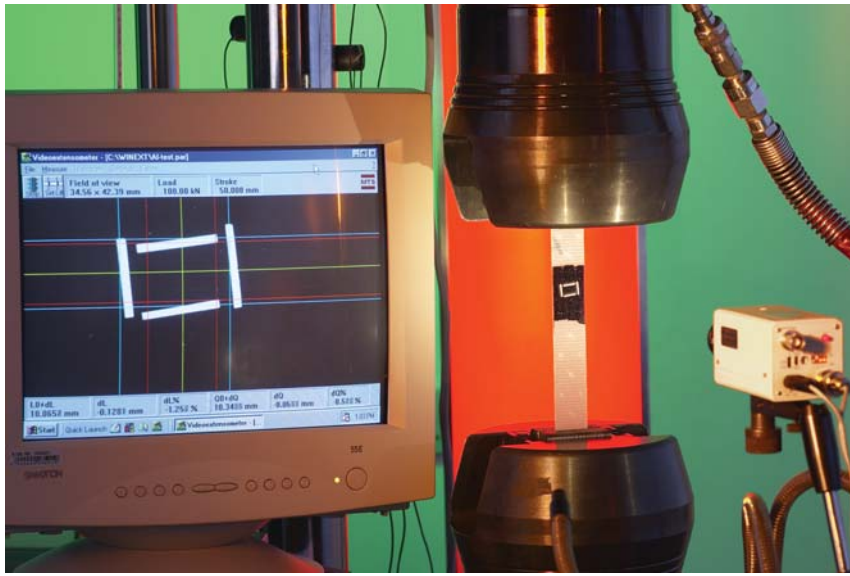

Figure 10 Tensile test set-up with measurement of longitudinal and transverse strains by video extensometry.

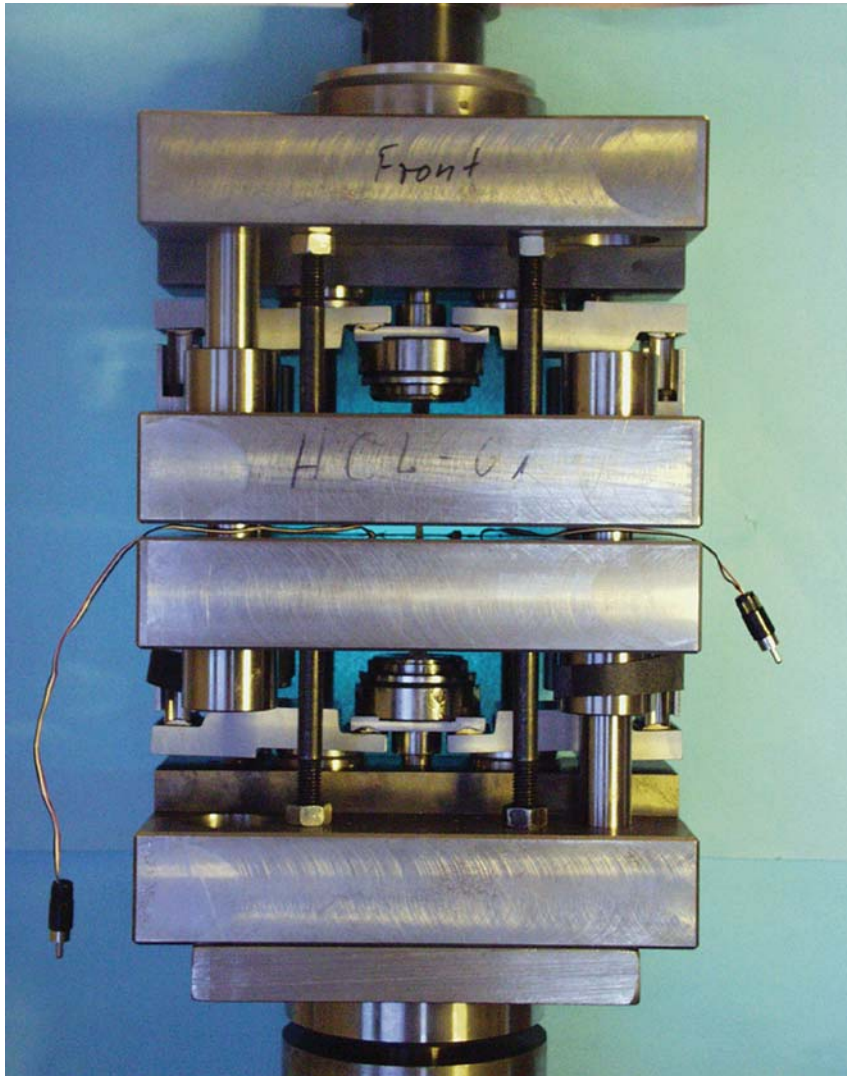

Figure 12 Advanced fixture for combined compression load transfer.

Figure 16 Thermoplastic composite rotorblade sections manufactured in a one-shot vacuum consolidation technique using the aluminum mold shown in the middle (92).

Annual Review of Materials Research
Volume 35, 2005

CONTENTS